Phase Space Hydrodynamics of Equivalent Nonlinear Systems: Experimental and Computational Observations

H. L. Berk, C. E. Nielsen, and K. V. Roberts

Citation: Physics of Fluids **13**, 980 (1970); doi: 10.1063/1.1693039
View online: http://dx.doi.org/10.1063/1.1693039
View Table of Contents: http://scitation.aip.org/content/aip/journal/pof1/13/4?ver=pdfcov
Published by the AIP Publishing

Articles you may be interested in

Phase space method for identification of driven nonlinear systems
Chaos **19**, 033121 (2009); 10.1063/1.3207836

Phase space observables and isotypic spaces
J. Math. Phys. **41**, 5883 (2000); 10.1063/1.1286986

Space qualification of an experimental two-phase flow thermal management system
AIP Conf. Proc. **217**, 1175 (1991); 10.1063/1.40083

Computing Problems in Nonlinear Hydrodynamic Stability
Phys. Fluids **12**, II-155 (1969); 10.1063/1.1692431

Metrization of Phase Space and Nonlinear Servo Systems
J. Appl. Phys. **24**, 38 (1953); 10.1063/1.1721128

This article is copyrighted as indicated in the article. Reuse of AIP content is subject to the terms at: http://scitationnew.aip.org/termsconditions.
Downloaded to IP: 132.239.66.164 On: Mon, 01 Feb 2016 01:41:07

Phase Space Hydrodynamics of Equivalent Nonlinear Systems: Experimental and Computational Observations

H. L. BERK
Lawrence Radiation Laboratory, University of California, Livermore, California
C. E. NIELSEN
Ohio State University, Columbus, Ohio and *Oak Ridge National Laboratory, Oak Ridge, Tennessee*
AND
K. V. ROBERTS
Culham Laboratory, Abingdon, Berkshire, England
(Received 14 February 1969; final manuscript received 15 September 1969)

The one-dimensional Vlasov equation describes the behavior of an incompressible self-interacting classical fluid which moves in the (q, p) phase plane. This type of phase fluid occurs in many physical problems and its hydrodynamic properties can be examined from a general point of view. A characteristic feature with initially unstable spatially homogeneous configurations is the development of stable nonlinear phase structures. Such examples occur as the result of the gravitational Jeans instability, or the two-stream and negative-mass instabilities of charged-particle beams. These structures can be related to one another by extending a duality principle due to Dory. The stable cavities in phase space which have been observed in numerical calculations on the two-stream instability are compared with stable proton clusters which develop from the negative-mass instability in the mirror experiment DCX-1.

I. INTRODUCTION

The evolution of a collisionless, classical many-body system, involving a long-range Hamiltonian interaction between the particles, can be described by a distribution function $f(q_i, p_i, t)$ in $2n$-dimensional phase space, where n is the number of spatial dimensions and (q_i, p_i) are the canonical coordinates and momenta. This function satisfies a Vlasov equation of the general form[1,2]

$$\frac{df}{dt} \equiv \left(\frac{\partial}{\partial t} + q_i \frac{\partial}{\partial q_i} + p_i \frac{\partial}{\partial p_i}\right) f = 0. \qquad (1)$$

A clear physical picture of the solution of Eq. (1) can be obtained, especially for problems requiring only one space dimension, by imagining $f(q_i, p_i, t)$ to be the density of an incompressible, self-interacting phase fluid which flows in the (q_i, p_i) phase space.

Vlasov's equation can be applied to a number of problems in plasma physics[3,4] and stellar dynamics[5] (for example, a galaxy can often be treated as a collisionless gas of stars), and also to electron tubes, microwave devices,[6] and particle accelerators[7] where space-charge effects are important. There is an extensive literature on the equilibrium solutions of the equation, which evidently correspond to stationary flows of the fluid in phase space, and also on the many linearized waves and instabilities which can be superimposed on these equilibria.[3,4] But, it would clearly be of interest to develop a general hydrodynamic theory for this type of classical fluid, capable of treating nonlinear and turbulent flows.

In this paper we should like to discuss some elementary physical principles which appear to underlie the nonlinear behavior of phase fluids in the simplest case $n = 1$ when the motion can be followed in the (q, p) plane. Starting from initial configurations which are fairly uniform but unstable, computer calculations[8] have demonstrated the formation of large-scale persistent structures in the phase plane. These have been seen in a variety of problems such as the two-stream instability,[9,10] the negative-mass instability,[11] and the gravitational Jeans instability.[12] There is also evidence for such structures in actual experiments with the Brookhaven Cosmotron[13] and the Oak Ridge DCX-1 mirror machine,[14,15] where in each case it is the negative-mass instability that occurs. Although these three instabilities may at first appear unrelated, we shall develop a nonlinear description that applies equally to all of them, and compare our computer results with some of the experimental observations.

A. Self-Interacting Phase Fluid

Vlasov's equation is formally the same as Liouville's equation for a single dynamical system with n degrees of freedom. However, it is necessary to emphasize that there is a considerable physical difference between the two cases. In the Liouville theory, f represents a probability distribution for a single system (or a frequency distribution for a large number of identical noninteracting systems),

This article is copyrighted as indicated in the article. Reuse of AIP content is subject to the terms at: http://scitationnew.aip.org/termsconditions. Downloaded to IP: 132.239.66.164 On: Mon, 01 Feb 2016 01:41:07

and the Hamiltonian $H(q_i, p_i, t)$ is a prescribed function of its arguments which is independent of f. In the Vlasov theory, f may be thought of as a coarse-grained density average over a macroscopic region in phase space, containing a large number of particle points, and it has much the same physical status as the hydrodynamic density ρ of a fluid which is actually composed of individual molecules. The Hamiltonian H is now a functional of f since it depends on the self-consistent potential Φ, which at each instant is to be calculated from the charge density of the phase fluid by solving Poisson's equation.

B. Step-Function Model

In any real physical problem the density $f(q, p)$ will vary smoothly over the phase plane, although it follows from Liouville's theorem that the density of each individual element of the moving phase fluid and the phase space area occupied by the element must remain invariant with time. However, because the nonlinear behavior of a system is often determined more by the over-all structure of the distribution function than by its precise details, it is useful to choose for $f(q, p)$ a step function that consists of a finite number of regions of $f = F_i \equiv$ constant as in Figs. 1 and 2. The state of the system at time t is then completely defined by specifying the boundary curves $C_i(t)$ between the different regions. Given this instantaneous configuration, one can calculate the self-consistent velocity components $\dot{q}$ and $\dot{p}$ at each point on the boundary curves, and so increment the system in time.

To study nonlinear phenomena in phase space in their simplest form one can go further, and just assume that $F = 1$ in some regions, and $F = 0$ elsewhere.

C. A Hydrodynamic Analogy

One can usefully compare a charged-particle phase fluid (where q is the spatial position x and p/m is the particle velocity v), with a two-dimensional liquid in a uniform gravitational field g. The kinetic energy of the charged particles

$$\tfrac{1}{2}m \iint v^2 f(x, v)\, dx\, dv \tag{2}$$

is analogous to the gravitational energy

$$g \iint y\, f(x, y)\, dx\, dy \tag{3}$$

of the liquid, where m is the electron mass, f the fluid density, and y the vertical coordinate. Because

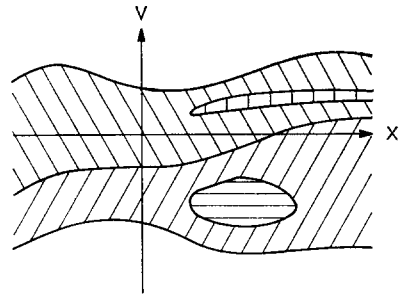

FIG. 1. A possible generalized step-function distribution. Each type of cross hatching represents a phase fluid with constant phase density. The evolution of the over-all system is determined solely by the dynamics of the boundaries separating incompressible fluid regions.

the motion is incompressible there is an invariant function $A(f)$, where $A(f)\, df$ is the total area occupied by fluid with density between f and $f + df$. If the density within a fluid region satisfies

$$\frac{\partial f}{\partial v^2} \leq 0 \tag{4}$$

or

$$\frac{\partial f}{\partial y} \leq 0, \tag{5}$$

respectively, then the region cannot release any free energy[16,17] to drive the system unstable. However, if there exist regions where the reverse inequality applies, then these tend to be unstable, and the fluid tries to find its own level, the charged particles giving up energy to the electrostatic field, and the liquid converting gravitational potential energy into kinetic form. This analogy is enhanced by plotting v^2 as the vertical coordinate, in which case light phase fluid tends to rise and heavy fluid to fall.

The step-function model of a phase fluid which has also been called the water bag model by De Packh,[18] corresponds to a standard assumption used in ordinary incompressible hydrodynamics, where it is convenient and physically natural to work with a liquid of uniform density wherever possible. When several f values are present in the Vlasov system,

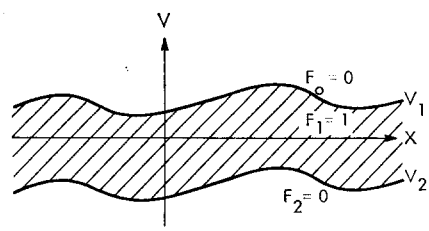

FIG. 2. Simplest phase fluid description of a one-dimensional gravitational strip or negative mass system. The phase fluid is a single strip of constant F surrounded on either side by $F = 0$ regions.

This article is copyrighted as indicated in the article. Reuse of AIP content is subject to the terms at: http://scitationnew.aip.org/termsconditions. Downloaded to IP: 132.239.66.164 On: Mon, 01 Feb 2016 01:41:07

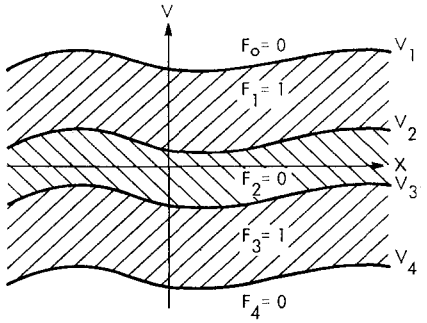

FIG. 3. Simplified description of a two-stream instability. The dynamics of the unstable modes are primarily governed by the boundaries separating the F_2 strip. The outer curves enclosing the $F_{1,3}$ regions only react passively to the inner ones and induce Debye screening.

the stable configuration of stratified layers with f a decreasing function of v^2 is quite analogous to a liquid system such as oil floating on water.

Oscillations in both the phase fluid and the liquid arise from energy changes due to distortion of the boundary curves. If $\partial f/\partial v^2 < 0$, only stable plasma oscillations can be supported and these are similar in many respects to stable gravitational waves, for example, on the surface of water or at the interface between two fluids of different density. On the other hand, if $\partial f/\partial v^2 > 0$ as in the two-stream instability, we have a situation which corresponds to the Rayleigh–Taylor instability of a liquid boundary.

It should, however, be stressed that although this hydrodynamic analogy is useful, it is not exact, and it should not be confused with a more formal vortex analogy which is briefly mentioned in Sec. V.

D. Applications of the Model

The step-function model of the Vlasov equation, which corresponds to

$$A(f) = \sum_k A_k \, \delta(f - F_k), \tag{6}$$

has been used several times in the past, often independently, for both theoretical and computational investigations on a range of different physical problems.

Nielsen, Sessler, and Symon[7] used such a model as one approach to a linear stability analysis, to show that the negative-mass instability can arise in high-energy particle accelerators. In their case q is an angular coordinate θ about the machine, and p is a suitably normalized angular-momentum variable. As has been mentioned, these instabilities are expected to evolve into the persistent nonlinear states which have been observed in the Cosmotron[13] and DCX-1.[14,15] Dory[10] treated the negative-mass instability numerically, and found that the proton phase fluid clustered together in agreement with the experiments.

Hohl and Feix[12] studied the relaxation of a one-dimensional, nonequilibrium gravitational system, and showed that the bulk of stars eventually form a stable equilibrium cluster. Finally, Berk and Roberts[9] treated a two-stream plasma instability where two interpenetrating electron beams comprise the $F = 1$ region, and enclose a uniform $F = 0$ region (see Fig. 3). In this case the $F = 0$ regions coalesce into an array of persistent structures of roughly elliptical shape. These regions of reduced density in (p, q) space will be referred to as cavities or holes. In these two problems the canonical coordinates are just the usual particle position and velocity.

E. Duality Principles

To explain these physical similarities, we shall extend a duality principle first proposed by Dory,[19] and in Sec. II show that the mathematical descriptions of all these systems are almost identical. Dory exhibited a formal duality between the negative-mass instability and the $F = 0$ region of the two-stream problem. The dynamics of these two systems are invariant to a mathematical transformation that maps one system into the other; namely, a simultaneous change of the sign of the mass, and an interchange of the $F = 0$ and $F = 1$ regions in phase space. In a similar way, the gravitational and negative mass systems are dual to each other by virtue of a simultaneous change in sign of both the mass and the force.

There is evidently some slight lack of correspondence, because the two outer $F = 0$ regions of the gravitational and negative-mass problems transform into $F = 1$ regions that extend to $v = \pm\infty$ in the two-stream problem. However, we can, in fact, show that the two outer curves of the two-stream problem play only a limited role. To a good approximation, they merely exert a screening effect on the Coulomb fields of the holes, modifying the attraction by a factor $\exp(-\kappa x)$, where $\kappa = \omega_p/\bar{v}$ corresponds to the Debye wavenumber, $\omega_p = (4\pi ne^2/m)^{1/2}$ is the plasma frequency, and $\bar{v}$ is the thermal spread. The nonlinear behavior of the unstable distribution can, therefore, be rather accurately related to that of a single gravitating strip, with Poisson's equation replaced by

$$\frac{d^2\Phi}{dx^2} - \kappa^2\Phi = 4\pi\rho. \tag{7}$$

This article is copyrighted as indicated in the article. Reuse of AIP content is subject to the terms at: http://scitationnew.aip.org/termsconditions. Downloaded to IP: 132.239.66.164 On: Mon, 01 Feb 2016 01:41:07

With the help of these duality principles, we see that the large-scale hole structures that develop in the nonlinear two-stream problem (Fig. 4) can be interpreted in several different ways. For example, it is found, perhaps somewhat surprisingly, that holes of like (positive) charge attract each other. We can explain this phenomenon first of all by realizing that the boundaries of the holes are determined by negatively charged electrons, and that these are indeed attracted toward neighboring positively charged regions. Secondly, the holes have an effective negative mass and hence must move in the opposite direction to the applied force. Finally, because of the duality principle, the holes behave as gravitational bodies which attract one another through a Debye-shielded Coulomb force.

F. Structure of the Paper

The various duality principles are discussed in more detail in Sec. II, where it is also shown how the unstable configurations are related to stable wave phenomena such as plasma oscillations. In Sec. III we discuss the experimental situations in which persistent nonlinear structures have been observed, and examine to what extent they can be approximated by our phase fluid model. Section IV interprets and compares the nonlinear structures observed in DCX-1 and the Cosmotron with the nonlinear phase space structures that arise in computations with the two-stream instability.

In the concluding section we indicate how the theoretical model can be used in general statistical,[20] thermodynamical,[16] and energetic[17] descriptions of phase-space fluids. Further, we briefly mention the close analogy that exists between the motion of an incompressible phase-space fluid and the two-dimensional vortex flow of an incompressible hydrodynamic fluid.

II. DUALITY PRINCIPLES

The duality between the two-stream instability and the negative-mass instability was first shown by Dory.[19] Because the Jeans instability of a one-dimensional gravitational system is also dual to the two-stream, and is the easiest to envisage physically, we first consider the equations for a gravitational phase fluid whose distribution is shown schematically in Fig. 2. The fluid has density $F = 0$ in regions 0 and 2, and $F = 1$ in region 1. The particle density $\rho(x)$ is determined by integration with respect to v, and depends only on the position of the boundary curves. Provided that the two curves $v_i(x)$ are single-valued, the density is

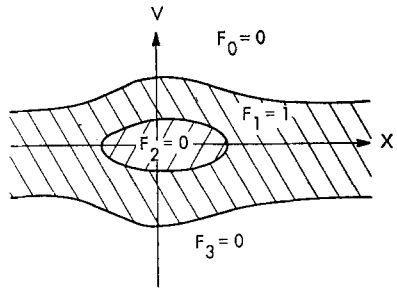

FIG. 4. Schematic diagram of a hole equilibrium. Each boundary contour coincides with a constant energy contour.

$$\rho(x) = \frac{n_0}{2\bar{v}} \sum_{i=1}^{2} \Delta f_i \, v_i, \tag{8}$$

where $\Delta f_i = F_i - F_{i-1}$ is the discontinuous jump in f at a boundary, and n_0, $\bar{v}$ are normalization factors for the density and thermal velocity, respectively.

The boundary curves move according to

$$\frac{dv_i}{dt} \equiv \left(\frac{\partial}{\partial t} + v_i \frac{\partial}{\partial x}\right) v_i = -\frac{\partial \Phi}{\partial x}, \tag{9}$$

where Φ is a normalized potential determined by Poisson's equation

$$\frac{\partial^2 \Phi}{\partial x^2} = \frac{4\pi\gamma^2 \rho}{m} = \frac{4\pi\gamma^2 n_0}{m} \sum_{i=1}^{2} \Delta f_i \, v_i. \tag{10}$$

Here, γ is the gravitational charge ($\gamma^2 = Gm^2$, where G is the universal gravitational constant), and m is the mass of the particles comprising the phase fluid.

In addition to the linearized Jeans instability predicted by Eqs. (9) and (10), one may also consider the equilibrium and stability of an isolated clump of phase fluid, that is, a one-dimensional star cluster. Provided that the initial gravitational energy is greater in absolute magnitude than the kinetic energy, such a cluster can never entirely disintegrate; some of the fluid may escape but some must always remain. On the other hand, it follows from the virial theorem that in a true equilibrium the magnitude of the potential energy must be exactly twice the kinetic energy,[21] and one is, therefore, led to examine how the system evolves if this condition is not satisfied.

This problem has been solved by Hohl and Feix[12] who calculated the shapes, in phase space, of gravitational equilibria formed from uniform-density phase fluid, and also carried out computer experiments which show how these equilibria develop from arbitrary initial configurations. If the initial state is near an equilibrium, thin streams of phase fluid are ejected from the boundary, and rotate in a clockwise direction about the center of the clump,

This article is copyrighted as indicated in the article. Reuse of AIP content is subject to the terms at: http://scitationnew.aip.org/termsconditions. Downloaded to IP: 132.239.66.164 On: Mon, 01 Feb 2016 01:41:07

giving rise to an apparent vortex motion. The clockwise motion occurs because stars on the right-hand side of the phase plane are attracted to those on the left, and so their velocity must decrease. They thus move downward, and eventually to the left. Similarly, stars on the left move upward, and eventually to the right. Because the fluid that has escaped has greater energy than the average, it lowers the energy density in the main clump, bringing it nearer to equilibrium. In the final state, the outer boundary of the clump has a roughly elliptical shape, which corresponds to a stationary particle orbit, and the clump is surrounded by very thin spiral arms of ejected material. This process is closely analogous to the cooling of a liquid by evaporation, leading to a two-phase equilibrium.

Now consider a fluid with an electronic interaction. The interaction constant transforms as $\gamma^2 \rightarrow -e^2$, but there are two ways in which the Eqs. (9) and (10) can remain invariant: either m must change sign (negative-mass instability), or Δf_i must change sign (two-stream instability).

In their linear analysis of the negative-mass instability Nielsen, Sessler, and Symon obtained equations for the step function distribution equivalent to Eqs. (9) and (10) in the frame moving with the mean speed of the particles, and where the mass is negative and is given by

$$m = \frac{1}{\omega R^2}\frac{\partial E}{\partial \omega}, \tag{11}$$

E being the energy of the particles in the beam, ω the angular frequency, and R the radius of the orbit. Dory[10] carried out a nonlinear computer calculation for this instability, and showed that the proton phase fluid condensed into a stationary cluster, a configuration equivalent to the gravitational cluster obtained by Hohl and Feix.

The situation is slightly more complicated for the two-stream instability (see Fig. 3), since to change the sign of Δf_i we must exchange the $F = 0$ and $F = 1$ regions. This system will be the dual of the others, only to the extent that the outer $F = 1$ regions of the equivalent gravitational system do not play a role in the dynamics.

It is now shown that this assumption is valid if the velocity width of the plasma is much larger than that of the cavity. If a uniform positive neutralizing background is assumed, so that the self-consistent equations of motion are Eq. (9) and Poisson's equation

$$\frac{\partial^2 \Phi}{\partial x^2} = -\omega_p^2\left(\sum_{j=1}^{4}\frac{v_j\,\Delta f_j}{2\bar{v}} - 1\right), \tag{12}$$

then if v_1 and v_4 are far removed from v_2 and v_3, particles moving on the two outer curves 1 and 4 should respond adiabatically to the potentials set up by the inner curves 2 and 3. Neglecting the term $\partial/\partial t$ in Eq. (10) for these outer curves, we find that

$$\frac{v_{1,4}^2}{2} + \Phi(x) = E_{1,4}, \tag{13}$$

where $E_{1,4}$ are the energies of the particles on the outer curves, which in this approximation are independent of x and t. If it is assumed that

$$\frac{v_{1,4}^2}{2} \gg \Phi(x),$$

then

$$v_{1,4} \simeq \pm(2E_{1,4})^{1/2}\left(1 + \frac{\Phi(x)}{2E_{1,4}}\right). \tag{14}$$

If this expression is substituted into Eq. (10), and the first term is used to cancel the neutralizing background, Eq. (12) becomes

$$\frac{\partial^2 \Phi}{\partial x^2} - \kappa^2\Phi = \frac{\omega_p^2}{2\bar{v}}\sum_{2}^{3}(-\Delta f_i)v_i, \tag{15}$$

where

$$\kappa^2 = \frac{\omega_p^2}{2\bar{v}}\left(\frac{1}{\bar{v}_1} + \frac{1}{|\bar{v}_4|}\right) \quad \text{and} \quad \bar{v}_{1,4} = \pm(2E_{1,4})^{1/2}.$$

(If $\bar{v}_1 = |\bar{v}_4|$, then $\bar{v} \simeq \bar{v}_1$ and $\kappa^2 = \omega_p^2/\bar{v}^2$ is the square of the Debye wavenumber.)

Equations (9) and (15) thus represent a description of the two-stream system, in terms of the holes alone. They are the equations of a gravitating phase fluid, except for the presence of an extra shielding term $\kappa^2\Phi$. We, therefore, expect that in the nonlinear phase of the two-stream instability cavities should be bound by Debye-shielded Coulomb forces.

It should be pointed out that the gravitational behavior of holes in an electron phase fluid is an essentially one-dimensional effect. We have seen that the outer curves distort, in an attempt to neutralize and screen the charge density produced by a hole. Because the spatial scale associated with charge neutralization is a Debye length λ_p, cavities, whose equilibrium length λ_h is calculated to be smaller than λ_p when screening is ignored, remain essentially unmodified when screening is taken into account. On the other hand, if $\lambda_h \geq \lambda_p$ in the absence of screening, then the equilibrium is likely to be drastically modified or destroyed altogether when screening is introduced.

We now show that it is only for phase fluids whose x-space character is essentially one-dimen-

This article is copyrighted as indicated in the article. Reuse of AIP content is subject to the terms at: http://scitationnew.aip.org/termsconditions. Downloaded to IP: 132.239.66.164 On: Mon, 01 Feb 2016 01:41:07

sional, that λ_h can be guaranteed to be less than λ_p when the spread of the hole velocity is much less than the thermal velocity of the background plasma.

The Debye length is given by $\lambda_p \propto (\bar{v}/\bar{\rho}^{1/2})$ where $\bar{\rho}$ is the mean particle density, while the size of the hole (the Jeans length λ_h of the corresponding gravitational system), is given by $\lambda_h \propto (v_h/\rho_h^{1/2})$ where v_h is the mean spread of velocity across the hole, and ρ_h is the spatial density of the displaced plasma or of the equivalent gravitating fluid. If n is the number of velocity dimensions in the system, it follows that for a fixed phase space density $\bar{\rho} \propto \bar{v}^n$ and $\rho_h \propto v_h^n$, so that

$$\left(\frac{\lambda_h}{\lambda_p}\right)^2 = \left(\frac{v_h}{\bar{v}}\right)^{2-n}. \tag{16}$$

Thus, it is only for the one-dimensional case, $n = 1$, that we are guaranteed that $\lambda_h \ll \lambda_p$ if $v_h \ll \bar{v}$. The gravitational analogy can, therefore, only be applied to holes in one-dimension-like configurations. Further calculations are needed to study multidimensional structures.

Returning to the question of duality, we can envisage systems which are inverse to those already discussed. Dual systems are transformed into one another by changing the signs of two of the parameters e^2, Δf_i, and m. If only one of the signs were changed, clusters would repel one another, so that these systems would be stable in the homogeneous state of Fig. 2. For an electron phase fluid with this configuration, e^2, Δf_i, and m are all positive, and perturbations lead to stable plasma oscillations. A gravitational example that is dual to these plasma oscillations is provided by the rings of Saturn. Here, $e^2 \to \gamma^2 = -e^2$, while as a consequence of the conservation of angular momentum, the effective mass m is negative. Saturn's rings are, therefore, stable as Maxwell[22] showed. If there were holes in the rings, then $\Delta f_i \to -\Delta f_i$ and so these holes might cluster together. Perhaps a future space experiment may verify this.[23]

Table I lists the eight possible dual and inverse systems obtained by giving either sign to the three parameters. The relation between a disturbance and its inverse is similar to the relation between a gravitational wave on the surface of a fluid and a Rayleigh–Taylor instability, where again the two regions $\rho = \rho_0$, $\rho = 0$ have been interchanged.

TABLE I. Dual and inverse systems.

Δf	Sign of effective mass	e^2	Physical system
+	+	+	Plasma waves
−	+	+	Two-stream instability, holes[a]
+	−	+	Negative mass, clusters[a]
−	−	+	Negative mass, holes
+	+	−	Gravitational system[a]
−	+	−	?
+	−	−	Saturn's rings
−	−	−	Holes in Saturn's rings[a]

[a] Dual systems, unstable in the homogeneous configuration.

III. EXPERIMENTAL INFORMATION AVAILABLE

Persistent nonuniform structures can be expected to arise in any of the unstable systems listed in Table I, but so far as we are aware, they have only been seen experimentally in devices using circulating particles, and nearly all the observations relate to the negative-mass instability. Although multistream instabilities do occur in linear devices, these are usually inconvenient for the observation of persistent structures, because of the short time which elapses before the beams reach the end of their path and any moving structure is destroyed. In principle, it would be possible to use a linear device with two equal and oppositely directed beams, as in the computer calculation of Fig. 5, so that the center of mass remained at rest. However, even this is less advantageous than the use of circulating beams.

There is one experiment on a circulating electron beam in a fixed-field betatron in which persistent signals were observed when $d\omega/dE > 0$ so that the negative-mass instability was necessarily absent.[24] This may well have been an example of a multistream instability, leading to the formation of persistent cavities in phase space. Unfortunately, the experimental evidence to support this identification is lacking, and the effect could also be attributed to a resistive-wall instability. Even so this experiment is significant, since it demonstrates that some mode of collective behavior other than the negative mass instability can also lead to persistent nonlinear states.

Returning to the negative-mass instability, we note that most of the results have been obtained with protons, since, in general, the electron frequencies are so high that detailed oscilloscope observations become difficult. Two proton devices will be discussed, each of which has $d\omega/dE < 0$ due to a negative radial gradient of the magnetic field, $dB/dr < 0$. The first is the Cosmotron proton ac-

This article is copyrighted as indicated in the article. Reuse of AIP content is subject to the terms at: http://scitationnew.aip.org/termsconditions. Downloaded to IP: 132.239.66.164 On: Mon, 01 Feb 2016 01:41:07

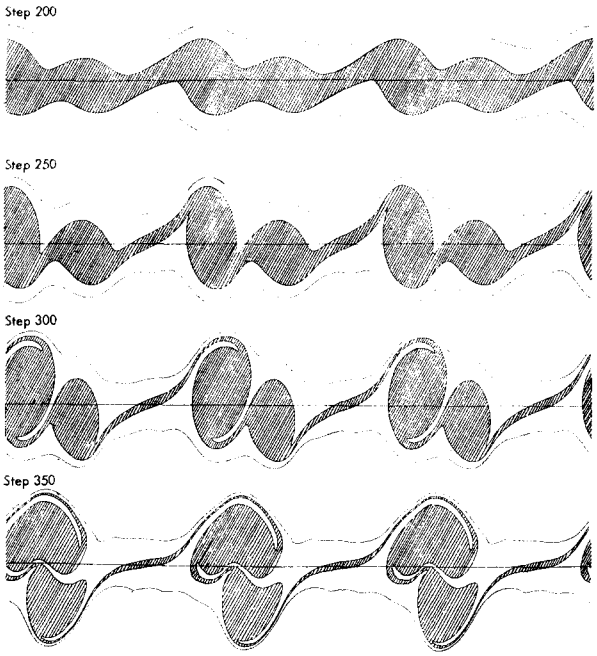

(a)

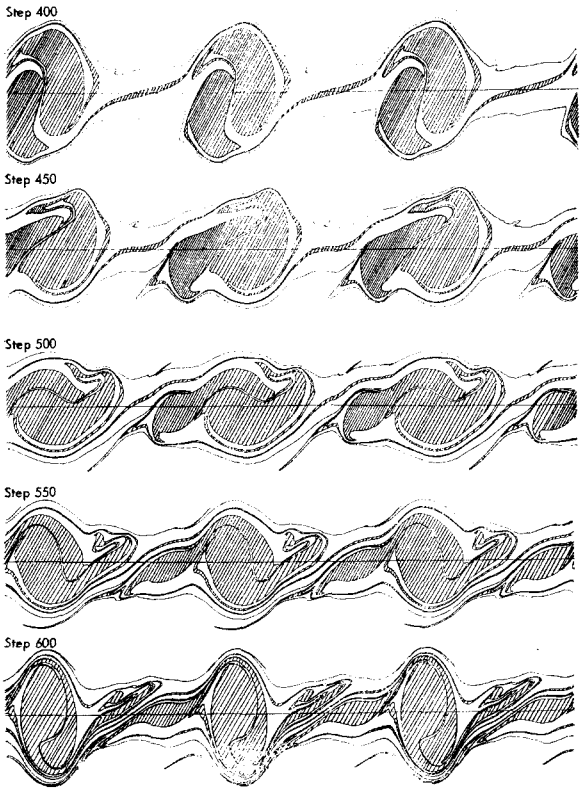

(b)

FIG. 5. The nonlinear development of a two-stream instability. The inner $F = 0$ region has been shaded to emphasize the development of hole structures.

celerator in which the negative-mass instability was first identified and reported in 1961,[13] and the second is the DCX-1 proton injection and trapping experiment.[14,15]

In both the Cosmotron and DCX-1 the protons produced stable clusters, bound together by their mutual repulsive forces. No essential role was played by the electrons. In the Cosmotron, the electron density was probably close to zero, and although electrons were present in DCX-1 and no doubt modified the electric fields of the proton clusters, they did not participate in the phenomena in a central way. A series of experiments[15] was carried out to verify this point. (Mirror traps such as DCX-1 do, of course, show other types of collective behavior in which the coupling between protons and electrons is crucial, but we do not discuss these modes here.)

There is a different relation between the potential and the charge distribution in these two devices. The ratio between the major and minor radii of the toroidal vacuum tube in the Cosmotron was large, and the proton ring can be approximated locally by a straight rod of charge, enclosed by a cylindrical conducting wall. Then, the potential $\Phi = g\sigma$ is proportional to the local linear charge density σ, where g^{-1} is the capacitance per unit length. In DCX-1 the entire proton ring was enclosed in a cylindrical vacuum vessel, and the potential at any point must, therefore, be obtained by integrating over the entire charge ring [this configuration was first analyzed by Fowler in an unpublished memorandum (see Ref. 15)]. The computer calculations used yet another relation between the potential and the charge, since the one-dimensional Poisson equation corresponds to infinite charge sheets. It might be thought that these differences would make comparisons difficult, but we believe that this is not the case. In the linear regime, the only theoretical difference between the two extreme cases of a variable line charge, and a set of infinite charge sheets, lies in the quantitative dependence of the instability threshold and growth rate on the wavenumber k. So far as nonlinear phenomena are concerned, the most significant feature, in all the systems that we have studied, seems to be that the Hamiltonian H is a functional of the density f in a two-dimensional phase space, and the exact form of this relationship is less important.

In both the Cosmotron and the DCX-1, normal operation involved continuous injection for a time much longer than the growth time of nonlinear states. For the experiments of interest here, how-

This article is copyrighted as indicated in the article. Reuse of AIP content is subject to the terms at: http://scitationnew.aip.org/termsconditions. Downloaded to IP: 132.239.66.164 On: Mon, 01 Feb 2016 01:41:07

ever, the proton input time was greatly reduced, in some cases to a time interval even shorter than the characteristic growth time for linear instability. In the Cosmotron the period during which nearly stationary states could be observed was usually limited by the slow increase of magnetic field required for synchrotron operation, while in DCX-1 the time was limited by charge exchange loss of the trapped protons. Strictly stationary states, signal generator modes with proton input equal to loss rate, could also be produced in DCX-1 by a suitable choice of operating conditions. This was, however, a special case that we only mention in passing to emphasize the great stability of nonlinear stationary configurations. Even with the more usual almost stationary situation, the variation from the constant phase density normally assumed in theory was too slow to disturb the comparison of the experiments with theory and numerical computation.

The experimentally measured quantity was the signal produced on an oscilloscope by protons passing a suitable detector, either of the linear charge density (Cosmotron), or of the electrostatic or magnetic field (DCX-1). We assume that in every case to be discussed here, the signal amplitude is approximately proportional to the charge per unit orbit length in the proton distribution.

IV. COMPARISON OF EXPERIMENTAL AND COMPUTATIONAL RESULTS

In this section we shall first relate the evolution of single clusters from a ring of charge, to the dual case of the evolution of holes from a gap in the phase space distribution. We then present examples of fully developed holes interacting.

In the computer experiments we investigated the two-stream instability shown in Fig. 5 and observed the formation of hole structures. For this experiment the distribution function for the spatially homogeneous equilibrium is characterized by

$$f(v) = \begin{cases} 1, & v_0/2 < |v| < v_0 \\ 0, & \text{(otherwise)} \end{cases}.$$

We employed periodic boundary conditions over a length L_p [in Fig. 5(a) three periodic intervals are shown], and perturbed the initial equilibrium with 16 random amplitudes and phases, i.e., the four longest waves on each curve. Other parameters for the equilibrium are

$$\frac{v_0\,\Delta t}{\Delta x} = \frac{1}{4}, \qquad \omega_p\,\Delta t = \frac{1}{20}, \qquad \Delta x = \frac{L_p}{64},$$

where Δx is the grid used for evaluating Poisson's equation. The unstable modes are $n = 1, 2$, where the wavenumber is $k = 2\pi n/L_p$, and the linear growth rates are $\gamma/\omega_p = 0.30, 0.315$, respectively.

The interaction of holes was studied numerically by preparing equilibrium hole structures and bombarding them at each other as in Fig. 6 and 7. In both figures $F = 1$ for the phase space fluid that lies outside the holes and within the outer contours, and $F = 0$ for the holes. In Appendix A we exhibit the analytic theory for the construction of an equilibrium hole from this type of distribution. In both figures there are 64 grid cells in the basic periodicity length and initially the x coordinates of the holes are centered at $x = 16\Delta x$ and $48\Delta x$. The potentials at $x = 0$ and $32x$ are chosen as zero.

In Fig. 6 the initial velocity v_c of the outer contours at $x = 0$ and $x = 32\Delta x$ is given by $v_c =$

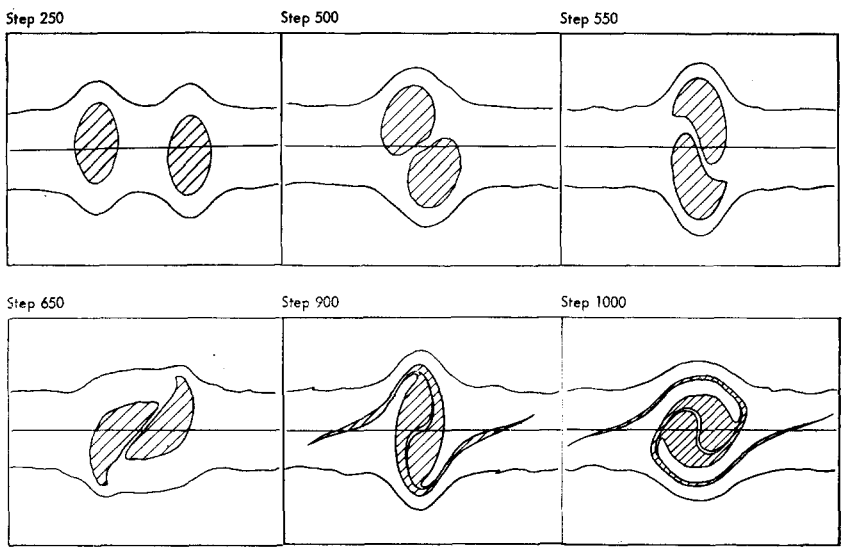

FIG. 6. An example of a hole–hole interaction when the relative velocity between holes is small. Hole attraction causes coalescence of the main bulk of the structures, together with a background spray from escaping regions.

This article is copyrighted as indicated in the article. Reuse of AIP content is subject to the terms at: http://scitationnew.aip.org/termsconditions. Downloaded to IP: 132.239.66.164 On: Mon, 01 Feb 2016 01:41:07

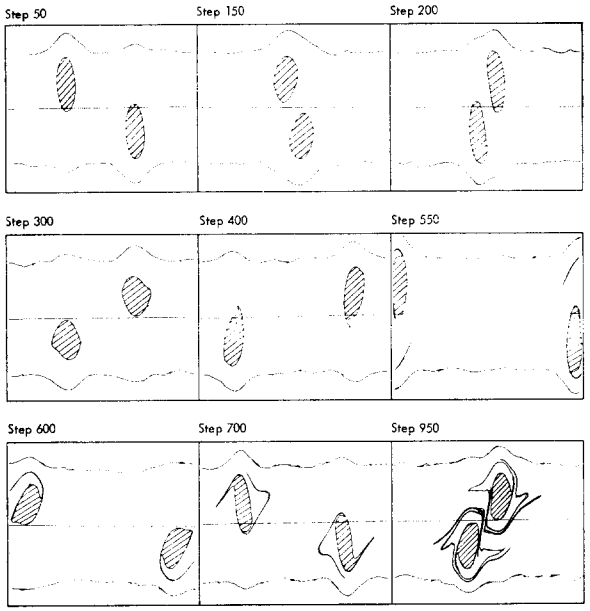

FIG. 7. An example of a hole–hole interaction when the relative velocity between holes is large. The holes pass through each other with some spray forming from "tidal" deformations.

$\pm\frac{5}{6}v_0$, and the holes initially move with velocities $v_h = \pm\frac{1}{6}v_0$ towards each other. The other parameters characterizing the equilibrium are $v_0\Delta t/\Delta x = 0.125$, $\omega_p\Delta x/v_0 = 0.337$, $\psi_0 = 0.5$ [see Eq. (A2) of the Appendix for definition of ψ_0].

In Fig. 7 the parameters characterizing the equilibrium are

$$\frac{v_c}{v_0} = \pm\frac{5}{3}, \qquad \frac{v_h}{v_0} = \pm\frac{2}{3},$$

$$\frac{v_0\,\Delta t}{\Delta x} = 0.125, \qquad \frac{\omega_p\,\Delta x}{v_0} = 0.426, \qquad \psi_0 = 0.1.$$

In comparing the experimental and computational results, it is to be kept in mind that two quite different frequencies occur in the experiments, the gyrofrequency ω_{ci} which characterizes the periodic motion of the charge cluster past the detector, and the much lower modulation frequency at which the amplitude of gyrofrequency signal varies during the time interval before the cluster reaches a stationary state. This modulation frequency is twice the frequency of phase space rotation of the nonstationary configuration. Only the phase space frequency appears in the computational results of Figs. 5 and 6, because the center of mass of the distribution is at rest in the coordinate system chosen. However, in Fig. 7 the holes traverse the periodic space and this traversal frequency is analogous to the gyrofrequency of the physical experiment.

A. Evolution of Clusters and Cavities

Figures 8 and 9 reproduce oscillograms, taken on two different shots, of the signal amplitudes of the gyrofrequency ω_{ci} and the second harmonic $2\omega_{ci}$ that developed after short pulses of injection into DCX-1. In each case, the injection was terminated before growth from the negative mass instability had perturbed the momentum or charge density appreciably. The phase density was, therefore, known initially, and was approximately uniform over phase angle, just as in the initial conditions for the computer run of Fig. 5.

The main objective of the DCX-1 experiment was to verify that the linear growth rate agreed with the one for the negative mass instability, and, indeed, satisfactory agreement was found.[15] However, at present we are primarily interested in the information that these experiments provide about nonlinear behavior. In general, after the charge density perturbation grows, at first exponentially, it reaches a limiting amplitude, and then it oscillates in ampli-

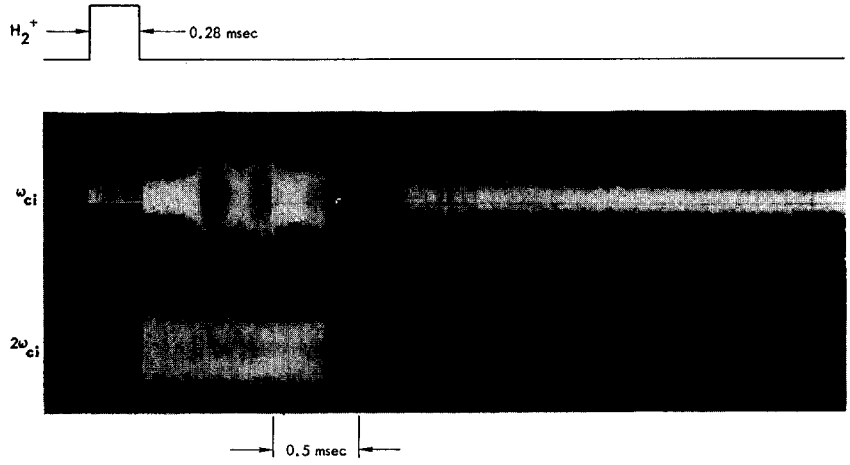

FIG. 8. Electrostatic signals from the Oak Ridge DCX-1 mirror machine which indicate the formation of a single cluster from the linearly stable regime. The modulation of the signal intensities is attributed to rotation in phase space of a cluster.

This article is copyrighted as indicated in the article. Reuse of AIP content is subject to the terms at: http://scitationnew.aip.org/termsconditions. Downloaded to IP: 132.239.66.164 On: Mon, 01 Feb 2016 01:41:07

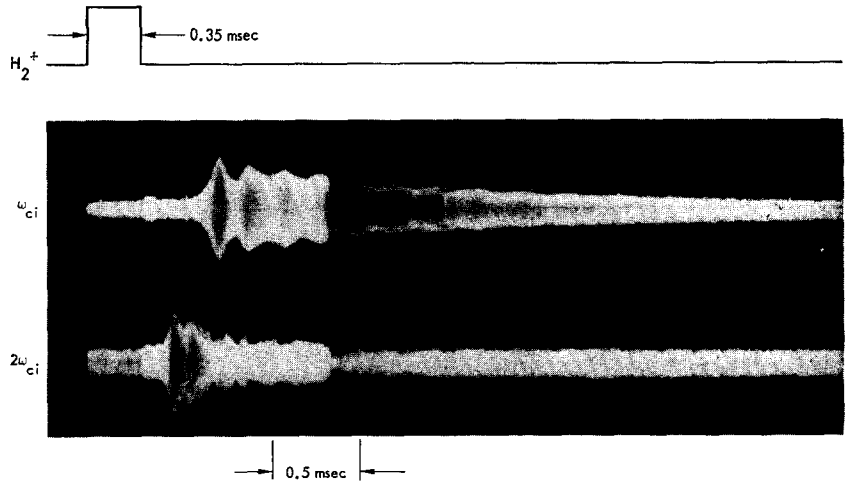

FIG. 9. Electrostatic signals from the Oak Ridge DCX-1 mirror machine which indicate the formation of two clusters from the linearly unstable regime. The second harmonic disappears and the first harmonic appears when two clusters coalesce into a single cluster.

tude while gradually decaying due to loss of trapped protons by charge exchange.

The simpler situation is that of Fig. 8 which shows a growth of signal amplitude at the gyrofrequency ω_{ci} only. We attribute this to the development of a single cluster in the charge ring, revolving about the magnetic axis. Figure 9 corresponds more closely to the computer run of Fig. 5, and here, we must assume that at first two clusters develop in the ring, producing a second harmonic signal as they revolve around the axis at the gyrofrequency, nearly at opposite ends of a diameter. Subsequently, they attract one another and coalesce into a single cluster, as indicated by the disappearance of the second harmonic and the emergence of the first harmonic. A corresponding coalescence occurs between step 250 and 400 of the computational results of Fig. 5.

In Fig. 5 we note that after the two cavities have grown and moved together toward coalescence by step 350 they have achieved maximum momentum spread Δp. As they continue coalescing and rotating about their common center they reach a position of minimum Δp near step 500 and a maximum again near step 600. Between step 350 and step 600 the line of maximum phase space distance across the configuration has rotated clockwise by approximately 180°. Maximum Δp extent of the cavity corresponds to maximum Δp in a charge cluster and consequently maximum local charge density and maximum experimental signal (the fact that phase space behavior of cavities and clusters may be equated is of course, merely an aspect of the duality discussed in Sec. II). Thus, steps 350 and 600 of Fig. 5 are to be placed in correspondence with the first two amplitude maxima in the first harmonic signal of Fig. 9. In general, the Δp maxima that occur as cavities or clusters of a nonstationary configuration rotate in phase space are represented by amplitude maxima in the experimental signal.

We now consider some quantitative aspects to further support our interpretation that the experimentally observed amplitude modulation is a manifestation of phase space rotation of a nonstationary configuration. First, we examine the relations between the initial growth time and nonlinear oscillation period in both the computational and experimental results. Second, we describe and discuss the experimental dependence of amplitude oscillation period upon cluster charge density.

From intuitive considerations one can expect that the phase space oscillation frequency should be comparable to the linear growth rate. As long as particles actually sample within a growth time essentially the same electric field phase as they would in linear theory this theory is accurate. However, linear theory must saturate when internal fields grow to a level that causes the phase of the particles to be significantly modified in a growth time. The internal fields have then also reached a level that produces phase space rotation at a rate comparable to the linear growth rate.

To illustrate this point we see that in Fig. 5 the first harmonic component of Δp has approximately doubled between step 250 and the first maximum at step 350, while the initial linear doubling time is about 50 steps. Since Δp maxima occur with a separation of 250 steps, we see that the doubling time during the final stage of initial growth is twice the linear time and about half the saturated amplitude oscillation period. Similar ratios hold for the experimental observation, as illustrated in Figs. 8 and 9. Measurements of the Fig. 8 oscillogram and other concurrent oscillograms give 0.33 msec as the amplitude oscillation period, 0.09 msec as the time from

This article is copyrighted as indicated in the article. Reuse of AIP content is subject to the terms at: http://scitationnew.aip.org/termsconditions. Downloaded to IP: 132.239.66.164 On: Mon, 01 Feb 2016 01:41:07

half-maximum to first maximum, and 0.04 msec as the small amplitude doubling time. The ratios of these times appear to be nearly independent of whether only a first harmonic grows from a small perturbation, as in Fig. 8, or whether it forms by coalescence of two second harmonic clusters as in Fig. 9, and are characteristic of all data.

In attempting to relate phase oscillation period to cluster charge density we confront the difficulty that the numerical dependence obviously depends upon the exact phase space configuration of the cluster in question. If, however, some reasonable assumption is made about the configuration of a cluster, it becomes possible to calculate how the ratios of the oscillation periods should depend upon the corresponding charge density ratios.

In the DCX-1 experiment the angular extent of the cluster remains constant at 2π, and we assume that the shape and spatial extent of the potential function are nearly unchanged during charge decay. It then follows that the oscillation time varies as the inverse square root of the maximum potential, just as the motion of a particle in a large-amplitude wave.

The experimental observations show that normally the amplitude modulation period increases monotonically as the mean signal amplitude decays. It is never possible to follow this increase in period to a very large ratio in amplitudes because the depth of the modulation soon becomes too small, even though the signal amplitude remains well above the noise level. Comparison of clusters formed following different injection pulses is of more uncertain significance because there is no assurance of similar cluster shapes. Nevertheless, for a given set of operating conditions the large-amplitude signals fairly consistently exhibit shorter amplitude modulation periods. Even over a change of more than a factor of 20 in charge input and loss rate (resulting from change in neutral pressure) the relation between amplitudes and periods is surprisingly uniform.

To illustrate numerically we again refer to Figs. 8 and 9. In Fig. 8 the modulation time T increases from 0.33 msec to 0.45 msec as the mean amplitude A decreases from 1.0 to 0.5 V at the oscilloscope (the signal at the pick-up loop is much less). In Fig. 9 (oscilloscope gain reduced) the time increases from 0.20 to 0.25 msec as the mean amplitude decreases from 1.9 to 1.4 V at the oscilloscope. Values of $A^{1/2}T$ in these four cases are 0.33, 0.32, 0.28, and 0.30. Thus, these examples, as well as most others done, show that the period varies as the square root of the amplitude.

The experimental decrease of amplitude modulation with time, until phase motion ceases to be observable, implies that the cluster approaches a stationary state in which the phase density is constant along every phase trajectory. In these experiments we find that, in general, the time required to reach a stationary state is of the order of 10 amplitude oscillation periods, i.e., five complete rotations of the phase space configuration. This decay may be ascribed to shearing of the phase fluid, as a consequence of the nonisochronous phase rotation resulting from the nonharmonic character of the potential well. This shearing is evident in all computer runs, and is even more conspicuous in Fig. 6 than in Fig. 5. Without nonisochronism in the rotation period, leading to the stretching and winding-up of phase fluid elements, there could be no approach to a true stationary state. The effect is particularly important when two structures coalesce, since a considerable amount of phase fluid is ejected and subsequently orbits in the field of the main body, and in Fig. 5 we see that the maximum in Δp at step 600 is already measurably less than at step 350.

We have thus seen that linear growth is succeeded, first by a nonlinear limit in which phase oscillations are directly observable as oscillating signal amplitudes, and then eventually by a metastable stationary state. The decay of this metastable state by particle loss due to charge exchange is, of course, a peculiarity of the DCX-1 experimental situation, and is not an intrinsic characteristic of the state itself.

B. Interacting Clusters and Cavities

It has been shown in Figs. 9 and 5 that two clusters or two cavities may fuse together, in the early stages of their evolution toward an eventual stationary state. A simpler example of a fusion event is shown in the computer sequence of Fig. 6. This differs from Fig. 5 in that two distinct fully developed equilibrium cavities were put in as an initial condition, so that their subsequent interaction could be studied independently of the complications of individual cavity evolution. We see that the cavities, which initially have a small relative velocity, attract one another and promptly merge into a single structure. Evidence of hole attraction can be obtained by observing that two noninteracting holes would take 768 steps to cross, while in Fig. 6 we see that two holes cross each other after 550 steps. Similar fusion events are observed experimentally with proton clusters.

In experiment, observations as simple as Fig. 6

This article is copyrighted as indicated in the article. Reuse of AIP content is subject to the terms at: http://scitationnew.aip.org/termsconditions. Downloaded to IP: 132.239.66.164 On: Mon, 01 Feb 2016 01:41:07

are, of course, difficult to obtain. Both the Cosmotron and DCX-1 start with an injection of a uniform ring of charge, and we have already interpreted Fig. 9 as showing that in DCX-1 strong interaction leads to fusion that is similar to the computer run of Fig. 5. In the Cosmotron, however, clusters interacted more weakly because of wall shielding and much greater spatial separation, so that there was time for many fully developed stationary clusters to form. From this multicluster state, which is partially similar to the initial state of Fig. 6, fusion of fully developed clusters occasionally occurred but, because of the weakness of the interaction, only when two happened to be very close together.

When the two structures have a greater relative velocity as in Fig. 7 they tend to distort each other but fusion is less likely to occur. In these figures we see evidence of hole attraction since it takes about 160 steps for the holes to cross each other instead of a free streaming time of 192 steps. Evidence of similar interaction has also been observed in two different experimental situations. In the Cosmotron, it was found that injection of two distinct momentum groups of protons resulted in two distinct groups of proton clusters that did not fuse, but did, in some cases, become coupled in pairs into closed phase-space orbits, each cluster retaining its identity and revolving about the other like the two individuals of a double star. See for example, Fig. 19 of Ref. 13. In this case, momentum in phase space is equivalent to radius in real space, so that viewed in the center-of-mass frame, the actual orbits resemble orbits in phase space.

A second situation in which clusters were observed to interact arose in DCX-1, when the two clusters were created by fission of a single large cluster. To clarify the experimental circumstances, first consider the growth of the single cluster shown in Fig. 10. In this case, injection continued long past the time of small-amplitude exponential growth, and we see in (a) an approximately linear growth of signal during charge input, particle trapping occurring both inside and outside the closed phase orbits of the cluster in an approximately constant ratio. When the input ceased, the signal decayed from particle loss, just as in Figs. 8 and 9.

If input had been continued at a suitably reduced level, the cluster could have been maintained in an exactly stationary state indefinitely. In fact, such constant-amplitude stationary-state signal-generator modes have been produced in DCX-1. When, however, input continued at the same level the result was as shown in Fig. 11; the cluster split into two

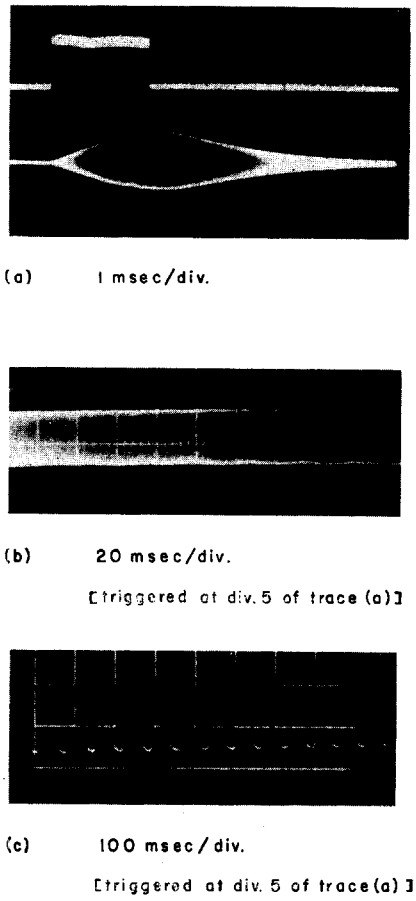

FIG. 10. Electrostatic signals due to the persistence of a single stable negative mass cluster in the Oak Ridge DCX-1 mirror machine. Upper trace in (a) indicates duration of input beam.

clusters with different gyrofrequencies that alternately moved into and out of phase, to produce the amplitude modulation shown in Fig. 11(b). When they were 180 deg out of phase, the two clusters produced the second-harmonic signal shown in Fig. 11(c), instead of a gyrofrequency signal as in Fig. 10(c).

The probable explanation for this cluster breakup, which is typical of DCX-1 observations, is that there is a limiting charge density above which a simple one-dimensional representation fails. As the charge density increases, the distribution spreads in the z direction parallel to the magnetic field because of the mutual repulsion of the protons. This spread moves the protons with larger z-oscillation amplitude toward the mirrors and so into regions of stronger magnetic field, and therefore, their average gyrofrequency increases. At the same time, the longitudinal spread weakens the azimuthal binding between the proton groups with larger and smaller z amplitudes. Eventually, when the coupling be-

This article is copyrighted as indicated in the article. Reuse of AIP content is subject to the terms at: http://scitationnew.aip.org/termsconditions. Downloaded to IP: 132.239.66.164 On: Mon, 01 Feb 2016 01:41:07

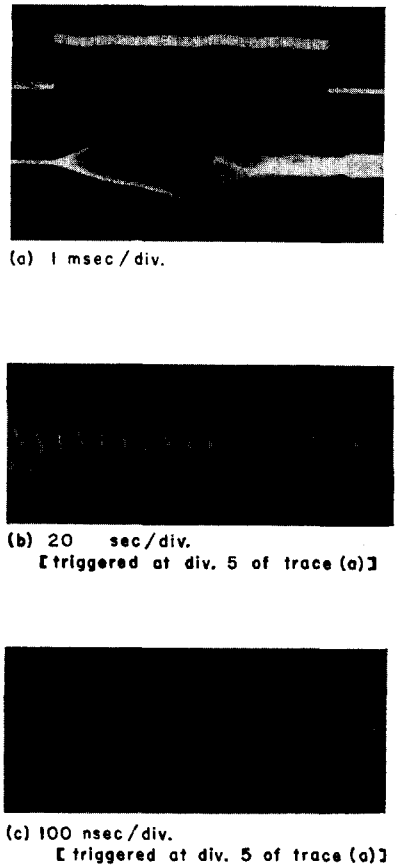

FIG. 11. Electrostatic signals due to the persistence of two negative mass clusters in the DCX-1 mirror machine. Initially only one cluster is present but above a critical density two clusters form.

comes too weak to hold the entire cluster together and force all the protons to revolve at a single frequency, the cluster splits into two, one consisting of the larger z-amplitude group with greater average gyrofrequency, and the other consisting of the smaller-amplitude lower-frequency group. In other experiments, a frequency increase during cluster growth followed by a splitting into two frequencies was observed with the spectrum analyzer, and was found to be characteristic of negative mass phenomena in DCX-1. For an example of frequency splitting see Fig. 9 of Ref. 14.

We now discuss the decrease of signal amplitude in Fig. 11, after the formation of two clusters. If only particle input and loss were involved, as in Fig. 10, we should expect the two clusters to grow individually at the same rate as before fission, since particle input continued. In fact, at a critical signal level the amplitude decayed in about 0.5 msec to a much smaller fluctuating level that never again, even though particle input continued, increased to the maximum reached by the well-organized single-cluster state before fission. We conclude that two or more clusters interacting may be mutually destructive. This experimental result is to be compared with the computer sequence of Fig. 7 in which two cavities of initially different average momentum, thus with some relative velocity, pass each other. The first pass occurs at approximately step 160 and the second at approximately step 900. At first, it appears that there is little effect, but before the end of the sequence considerable filamentation has occurred. The inelastic behavior of the collisions has somewhat modified the collision rate. If the hole encounters were elastic, the periodicity time would be 768 steps. As a result of inelastic collisions the holes lose energy, and as they are holes and not particles, speed up, so that the new traversal time is 740 steps. It is evident that the cavities will be modified substantially in a time that corresponds to the experimental decay time of 0.5 msec for cluster disintegration. During the experimental decay interval, input and loss processes changed the proton density only very slightly, so that for purposes of comparison with the constant-phase-density computer case the experimental situation may be viewed as likewise a constant-density case.

In brief, the consequences of the interaction between two clusters or two cavities depend upon their relative phase-point momenta. When the average momenta are nearly equal, they attract and fuse into one structure; the most stable configuration is a single cluster or cavity. When their momenta are sufficiently different, they pass without much mutual disturbance, or in some cases form a bound structure with separate identities retained. When their momenta differ too much to allow fusion and too little to make mutual disturbance negligible, they tend to destroy each other.

V. CONCLUDING REMARKS

We have seen that a simple phase-fluid model of the Vlasov equation can be applied to several equivalent physical systems, and that it predicts nonlinear states which are similar to those that occur experimentally. Further insight into the dynamical behavior of many-body systems may be gained by applying general arguments involving energy, statistical mechanics, and thermodynamics. We briefly indicate some of these arguments here, and hope to present them in more detail in a later paper.

It can be shown that an equilibrium structure of a gravitational phase fluid is a minimum total energy state (so that any perturbation, under the constraint of over-all area conservation, increases the

This article is copyrighted as indicated in the article. Reuse of AIP content is subject to the terms at: http://scitationnew.aip.org/termsconditions. Downloaded to IP: 132.239.66.164 On: Mon, 01 Feb 2016 01:41:07

energy of the system), and that a negative-mass cluster and a hole in an infinite electron phase fluid are maximum total energy states. This guarantees the stability of each of these structures, since instability can only arise if the fluid can distort in a manner that conserves over-all energy; evidently no motion is permitted if the energy is an extremum.

With this constraint on the energy, one may ask how an equilibrium configuration is ultimately attained. The clue appears in Fig. 6, where we see the coalescence of two holes that have bombarded each other. The new excited state does not have the proper area–energy relation to enable the hole fluid to form a new equilibrium. Instead, it is necessary for the structure to get rid of excess (negative) energy by evaporating layers from its boundaries. This evaporated material then orbits in the attractive field of the main hole, and becomes more and more randomized as time goes on; eventually, the system appears to exhibit a two-phase thermodynamic equilibrium.

This picture certainly suggests that a new statistical formalism is needed, in order to describe the evolution of the holes and of background plasma. An appropriate form of statistical mechanics has recently been worked out by Lynden-Bell,[20] and one of the most interesting features is that individual elements of phase fluid obey a classical exclusion principle, since no two elements can occupy the same cell in phase space. The total energy is also conserved, and if there are only two types of region, $f = 0$ and $f = 1$, the Lynden-Bell distribution is the same as that of Fermi. Our numerical results are in good qualitative agreement with Lynden-Bell's theory when applied to the holes of the plasma system (rather than to the plasma itself), or equivalently to the phase fluid of a gravitational system, for which the theory was originally developed.

In actual experiments, and in more detailed theory, energy sources and sinks may be present that can cause perturbations to grow. Even in our two-stream calculation we may note that the hole configuration is strictly not a maximum total energy state, since it is possible to excite positive-energy plasma oscillations on the outer curves. However, since these have phase velocities which are quite different from those of the negative energy waves excited at the hole boundaries, the two types of waves do not couple effectively. Hence, in our computer experiment the holes are stable because the system cannot coherently transfer energy from the inner to the outer curves.

In other experiments, energy sinks for the holes may be more important. Morse and Nielson[25] recently performed a two-dimensional calculation of the two-stream instability and found that holes dissipate in the time that it takes thermal particles to cross their transverse dimension. Hence, one can probably only expect nonlinear hole structures to persist in systems where transverse motion is inhibited by a magnetic field. Another important aspect of the stability of nonlinear structures is their interaction with slow waves and dissipation mechanisms in the system, e.g., ion acoustic waves and Landau damping.

Much of the analysis of this paper can equally well be applied to the vortex motion of an incompressible two-dimensional hydrodynamic fluid. In this case the analog to the Vlasov equation is the equation which governs the advection of the vorticity $F = (\partial v_y/\partial x) - (\partial v_x/\partial y)$; i.e.,

$$\frac{dF}{dt} \equiv \frac{\partial F}{\partial t} + v_x \frac{\partial F}{\partial x} + v_y \frac{\partial F}{\partial y} = 0. \tag{17}$$

The two spatial coordinates x and y are canonically conjugate[26] to one another since they satisfy the relations

$$v_x = \dot{x} = \frac{\partial \psi}{\partial y}\,; \qquad v_y = \dot{y} = -\frac{\partial \psi}{\partial x}\,, \tag{18}$$

where the Hamiltonian ψ is just the velocity stream function. The velocity, therefore, behaves as an incompressible phase fluid, and it is only in the equation that determines ψ that the vortex system differs from the Vlasov problem. The stream function ψ is, in fact, determined by the two-dimensional Poisson equation

$$\frac{\partial^2 \psi}{\partial x^2} + \frac{\partial^2 \psi}{\partial y^2} = -F. \tag{19}$$

Since x and y now appear in a symmetrical way, general thermodynamic arguments are easier to use. Previous numerical studies of systems mathematically equivalent to Eqs. (18) and (19) (such as the Kelvin–Helmholtz instability or diocotron instability[27–31]) show that fluids with a sheared flow and with velocities initially independent of x, evolve into vortex structures. The x-y phase space disgrams are strikingly similar to our x-v diagrams in Fig. 5.

ACKNOWLEDGMENTS

We are indebted to the DCX-1 group for previously unpublished data, and in particular to Dr. J. L. Dunlap for supplying Figs. 8–11. Also, we would like to acknowledge the excellent services offered by the computer center of the University of

This article is copyrighted as indicated in the article. Reuse of AIP content is subject to the terms at: http://scitationnew.aip.org/termsconditions. Downloaded to IP: 132.239.66.164 On: Mon, 01 Feb 2016 01:41:07

California, San Diego, where the computations given in this paper were performed.

This work was performed jointly under auspices of the United States Atomic Energy Commission and the United Kingdom Atomic Energy Authority.

APPENDIX. HOLE EQUILIBRIA

Here, we construct analytically the hole equilibria that were used to form our initial states in the hole–hole simulation experiments. For our case both pulse solutions and wave trains (Bernstein–Greene–Kruskal[31] modes) exist. Although the formalism we present treats wave trains, the pulse solutions will be emphasized since in our problem the periodic solutions are essentially just a set of pulses stacked in an array.

In the wave frame the equilibrium contours in velocity space, shown in Fig. 12, are also contours of constant energy. As our origin we select a point where the velocity space contours peak and at the troughs we choose $\phi = 0$. The contours $C_{1,4}$ are then open-ended contours with velocity

$$v_{1,4}(x) = \pm\{2[E_{1,4} - \phi(x)]\}^{1/2},$$

while contours $C_{2,3}$ are of equal negative energy with velocity

$$v_{2,3} = \pm\{-2\,[|E_{2,3}| + \phi(x)]\}^{1/2}.$$

From Eq. (12) we then have

$$\frac{\partial^2\phi}{\partial x^2} \equiv \frac{1}{2}\frac{\partial}{\partial\phi}\left(\frac{\partial\phi}{\partial x}\right)^2$$

$$= -\frac{\omega_p^2}{2\bar{v}}\{[v_1^2 - 2\phi(x)]^{1/2} + [v_4^2 - 2\phi(x)]^{1/2} - 2\bar{v}$$

$$- 2[-v_2^2 - 2\phi(x)]\theta[-v_2^2 - 2\phi(x)]\}, \qquad \text{(A1)}$$

where

$$v_{1,4}^2 = 2E_{1,4}, \qquad v_2^2 = -2E_2$$

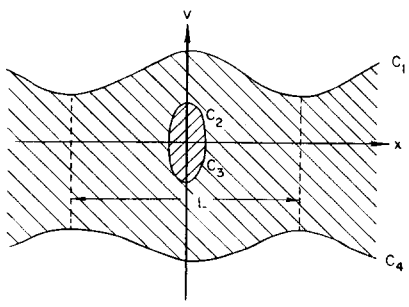

FIG. 12. Schematic phase space diagram used to obtain analytic equilibrium hole solutions.

and

$$\theta(x) = \begin{cases} 1, & x > 0 \\ 0, & x < 0 \end{cases}.$$

When we introduce the transformations

$$\psi = -\frac{2\phi}{\bar{v}^2}, \qquad y = \frac{\omega_p x}{\bar{v}}, \qquad \alpha_i^2 = \left(\frac{v_i}{\bar{v}}\right)^2,$$

and integrate Eq. (A1), we find

$$\left(\frac{\partial\psi}{\partial y}\right)^2 = \tfrac{4}{3}[(\alpha_1^2 + \psi)^{3/2} - (\alpha_1^2 + \psi_0)^{3/2}$$

$$+ (\alpha_4^2 + \psi)^{3/2} - (\alpha_4^2 + \psi_0)^{3/2}$$

$$- 2(\psi - \alpha_2^2)^{3/2}\theta(\psi - \alpha_2^2)$$

$$+ 2(\psi_0 - \alpha_1^2)^{3/2} - 3(\psi - \psi_0)], \qquad \text{(A2)}$$

where $\psi_0 = \psi(y = 0)$ which must be greater than zero.

From our assumptions, we have the constraints that $\partial\psi/\partial y$ vanish where $\psi = 0$ and the right-hand side of (A2) must be greater than zero between the zeros of $\partial\psi/\partial y$. The first constraint yields

$$\alpha_2^2 = \psi_0 - (\tfrac{1}{2})^{2/3}[(\alpha_1 + \psi_0)^{3/2} - \alpha_1^3$$

$$+ (\alpha_4 + \psi_0)^{3/2} - \alpha_4^3 - 3\psi_0]^{2/3}. \qquad \text{(A3)}$$

The second constraint also limits the choice of parameters, and for example, yields the condition $\alpha_1 + \alpha_2 \geq 2$. Further, the parameters cannot violate the condition $\alpha_2^2 > 0$.

If we choose parameters to satisfy all constraints, then from (A2) we can solve for ψ by quadrature and find

$$y = \int_{\psi}^{\psi_0} \frac{d\psi}{|d\psi/dy|}. \qquad \text{(A4)}$$

The condition for a single pulse is $\alpha_1 + \alpha_2 = 2$ since it then follows that for small $\psi(\psi \ll \alpha_{1,4}^2)$, $(\partial\psi/\partial y)^2 = \psi^2/\alpha_1\alpha_4$ and, therefore, from (A4) we see that $L \to \infty$. If we solve for ψ outside the hole when $\psi \ll \alpha_{1,4}^2$, we find

$$\psi = \psi_1 \exp\left(-\frac{|y - y_c|}{(\alpha_1\alpha_4)^{1/2}}\right), \qquad \text{(A5)}$$

where ψ_1 is a constant that can be determined from the exact solution of (A4) and y_c is the point where $\psi(y_c) = \alpha_2^2$ (if $\alpha_2^2 \ll \alpha_{1,4}^2$ then $\psi_1 = \alpha_2^2$). Hence, outside the hole, plasma shielding causes the potential to decay exponentially.

In preparing pulse equilibria for computer experiments, Eq. (A4) is integrated with $\alpha_1 + \alpha_2 = 2$.

This article is copyrighted as indicated in the article. Reuse of AIP content is subject to the terms at: http://scitationnew.aip.org/termsconditions. Downloaded to IP: 132.239.66.164 On: Mon, 01 Feb 2016 01:41:07

Once the potentials are known the velocity space contours can be formed. A negligible error arises near the ends of the pulse since in the computer experiments the pulse is of finite size.

[1] A. A. Vlasov, Zh. Eksp. Teor. Fiz. **8**, 291 (1938).
[2] L. D. Landau, J. Phys. (U. S. S. R.) **10**, 25 (1940).
[3] T. H. Stix, *The Theory of Plasma Waves* (McGraw-Hill Book Company, New York, 1962), p. 158.
[4] D. C. Montgomery and D. A. Tidman, *Plasma Kinetic Theory* (McGraw-Hill Book Company, New York, 1964), p. 51.
[5] K. F. Ogorodnikov, *Dynamics of Stellar Systems* (The MacMillan Company, New York, 1965), p. 137.
[6] V. N. Shevchik, G. N. Shvedov, and A. V. Sobleva, *Wave and Oscillatory Phenomena in Electron Beams at Microwave Frequencies* (Pergamon Press, Inc., New York, 1966), p. 66.
[7] C. E. Nielsen, A. M. Sessler, and K. R. Symon, in *Proceedings of the International Conference on High Energy Accelerators and Instrumentation* (Centre Européen de Recherches Nucléaires Scientific Information Service, Geneva, Switzerland, 1959), p. 239.
[8] Typical examples of recent computer calculations are found in the *Symposium on Computer Simulation of Plasma and Many Body Problems*, NASA SP-153 (Clearinghouse for Federal Scientific and Technical Information, Springfield, Virginia). This report includes an extensive bibliography of past calculations, compiled by C. K. Birdsall, p. 375. Also see Los Alamos Scientific Laboratory Rept. LA-3990 (1968).
[9] H. L. Berk and K. V. Roberts, Phys. Fluids **10**, 1595 (1967). K. V. Roberts and H. L. Berk, Phys. Rev. Letters **101**, 297 (1967).
[10] T. P. Armstrong, Phys. Fluids **10**, 1269 (1967).
[11] R. A. Dory, Bull Am. Phys. Soc. **8**, 378 (1963).
[12] F. Hohl and M. Feix, Astrophys. J. **147**, 1164 (1967).
[13] M. A. Barton and C. E. Nielsen, in *Proceedings of the Conference on High Energy Accelerators*, (United States Atomic Energy Commission, Washington, D. C., 1962), p. 163.
[14] J. L. Dunlap, G. R. Haste, C. E. Nielsen, H. Postma, and L. H. Reber, Phys. Fluids **9**, 199 (1966).
[15] H. Postma, J. L. Dunlap, R. A. Dory, G. R. Haste, and R. A. Young, Phys. Rev. Letters **16**, 265 (1966).
[16] C. S. Gardner, Phys. Fluids **6**, 839 (1963).
[17] T. K. Fowler, Phys. Fluids **7**, 249 (1964).
[18] D. C. DePackh, J. Electron. Control **13**, 417 (1962).
[19] R. A. Dory, J. Nucl. Energy, Pt. C, **6**, 511 (1964).
[20] D. Lynden-Bell, Monthly Notices Roy. Astron. Soc. **136**, 101 (1967).
[21] Reference 5, p. 181.
[22] J. C. Maxwell, *Scientific Papers* (Cambridge University Press, London, 1890), Vol. 1, p. 288.
[23] An effect of this kind can be seen in a recent computer film of a rotating system of gravitating stars, made by Dr. F. Hohl and presented at the Third Annual Symposium on the Numerical Simulation of Plasmas, Stanford (1969).
[24] F. E. Mills, C. D. Curtis, F. L. Peterson, C. A. Radmer, M. F. Shea, D. A. Swenson, and D. E. Young, Rev. Sci. Instr. **35**, 1451 (1964).
[25] R. L. Morse and C. W. Nielson, Phys. Fluids **12**, 2418 (1969).
[26] L. Onsager, Nuovo Cimento Suppl. **6**, 130 (1949).
[27] F. H. Abernathy and R. E. Kronauer, J. Fluid Mech. **13**, 1 (1962).
[28] J. A. Byers, Phys. Fluids **9**, 1038 (1966).
[29] R. H. Levy and R. W. Hockney, Phys. Fluids **11**, 766 (1968).
[30] C. K. Birdsall and D. Fuss, Bull. Am. Phys. Soc. **13**, 283 (1968).
[31] I. B. Bernstein, J. M. Greene, and M. D. Kruskal, Phys. Rev. **108**, 546 (1957).

THE PHYSICS OF FLUIDS VOLUME 13, NUMBER 4 APRIL 1970

Technique for Determining the Propagation Characteristics of Instabilities

D. A. LEE
Aerospace Research Laboratories, Wright-Patterson Air Force Base, Ohio
AND
G. K. SOPER
Air Force Institute of Technology, Wright-Patterson Air Force Base, Ohio

(Received 25 October 1968; final manuscript received 20 November 1969)

A method for obtaining an approximation to the large-time behavior of instabilities which are represented by multidimensional Fourier integrals of a type which arises in dispersion relation studies is discussed. Applications to moving striations, the beam-plasma instability, and to the ion-cyclotron resonance instability are given and the results compared with those of other methods.

I. INTRODUCTION

Propagation characteristics of instabilities have been discussed by several authors using an approximation in which the growth rate is replaced by its osculating parabola at an absolute maximum, and the frequency by its tangent line at that point.[1-3] In this paper we give an extension of this method to the treatment of instabilities $u(\mathbf{x}, t)$ which are represented by multidimensional Fourier integrals of the form

$$u(\mathbf{x}, t) = \int_{\mathbf{k}} g(\mathbf{k}) \exp [p(\mathbf{k})t + i\mathbf{k}\cdot\mathbf{x}] \, d\mathbf{k} \qquad (1)$$

and a discussion of the conditions under which this approximation leads to a correct asymptotic expansion in the sense of Poincaré. These conditions

This article is copyrighted as indicated in the article. Reuse of AIP content is subject to the terms at: http://scitationnew.aip.org/termsconditions. Downloaded to IP: 132.239.66.164 On: Mon, 01 Feb 2016 01:41:07